

Research Paper

Stability of freeze-dried products subjected to microcomputed tomography radiation doses

Tim Wenzel^{1,2}, Achim Sack³, Patrick Müller³, Thorsten Poeschel³,
Sonja Schuldt-Lieb⁴ and Henning Gieseler^{1,*} 

¹GILYOS GmbH, Würzburg, Germany

²Division of Pharmaceutics, Freeze Drying Focus Group, Friedrich-Alexander-Universität (FAU) Erlangen-Nürnberg, Erlangen, Germany

³Institute for Multiscale Simulation (MSS), Friedrich-Alexander-Universität (FAU) Erlangen-Nürnberg, Erlangen, Germany

⁴Medac GmbH, Wedel, Germany

*Correspondence: Henning Gieseler, GILYOS GmbH, Friedrich-Bergius-Ring 15, 97076 Würzburg, Germany. Tel: +49-931-90705678; Fax: +49-931-90705679; Email: info@gilyos.com

Received April 18, 2020; Accepted February 9, 2021.

Abstract

Objectives Microcomputed tomography (μ CT) is a powerful analytical tool for non-invasive structural analysis. The stability of drug substances and formulations subjected to X-ray radiation may be a concern in the industry. This study examines the effect of X-ray radiation on the stability of freeze-dried pharmaceuticals. The investigation is a proof of concept study for the safety of μ CT X-ray radiation doses during the non-destructive investigation of freeze-dried products.

Methods Different formulations of clotrimazole, insulin and l-lactate dehydrogenase were freeze-dried and the products exposed to a defined dose of radiation by μ CT. Conservative freeze-drying conditions were used. Irradiated and normal samples were analysed for their stability directly after freeze-drying and after stability testing.

Key findings The stability of model compounds was well maintained during freeze-drying. Some degradation of all compounds occurred during accelerated stability testing. The results showed no differences between the irradiated and normal state directly after freeze-drying and accelerated stability testing.

Conclusions No evidence of a detrimental effect of 100 Gy X-ray exposure on a model small molecule, peptide and protein compound was found while useful structural information could be obtained. Consequently, the technology may be useful as a non-destructive tool for product inspections if the formulation proves stable.

Keywords: freeze-drying; micro computed tomography; morphology; inspection; stability

Introduction

The freeze-drying process typically results in a highly porous product cake that can be rapidly reconstituted with the adequate solvent and administered to the patient. The process and product morphology are directly interconnected. The initial morphology of the ice crystal network is determined during the freezing step and can be influenced

by shelf temperature modifications or technologies that allow for control of the ice nucleation temperature.^[1,2] Ideally, this structure is maintained throughout the drying process by ensuring that the product temperatures are maintained below a product-specific critical formulation temperature. The consequences of exceeding this limit could, for example, be a loss of structure due to viscous flow

(collapse) or melt back of ice crystals.^[3] Because of the possible influence of structural defects on other product quality attributes such as active pharmaceutical ingredient (API) stability or reconstitution behaviour, these defects can present a risk for patient safety and drug efficacy. Acceptable appearance of freeze-dried products is an ongoing debate in the pharmaceutical industry and is usually defined for each product during product development.^[4]

Visual inspection of freeze-dried products is typically performed manually or semi-automatically by trained operators. An inherent problem of this approach is the inability to detect defects such as collapsed areas or meltback that may be confined to the inside of the product cakes as well as the possibility of human error during the inspection. Scanning electron microscopy can be a valuable asset during development to analyse the inner product morphology. Due to its destructive nature, large-scale investigations of a production batch are not feasible for this technique, however. Non-invasive techniques such as three-dimensional laser scanning or microcomputed tomography (μ CT) have gained attention for the structural analysis of freeze-dried products in the last years. Pisano *et al.*^[5] have demonstrated that μ CT data can be used to estimate pore sizes for freeze-dried products and used this information to model heat and mass transfer during the freeze-drying process. Haeuser *et al.*^[6] analysed freeze-dried cakes by μ CT and assessed the overall cake structure and defects confined to the product inside. They were able to derive macrostructural (e.g. cake volume) as well as microstructural information (e.g. collapsed areas with higher contrast due to a more dense structure) from μ CT data. Kunz *et al.*^[7] used μ CT data to describe the differences in the pore morphology and assess homogeneity or the presence of collapse areas for freeze-dried products formulated with different cosolvents. The advantages of these techniques over a macroscopic visual inspection include the ability of detecting defects confined to the inside of the products as well as quantifiable information on defect severity. Quantitative product defect information could allow these techniques to be used as an unbiased criterion for product morphology and possibly at one point fully automated product inspection processes.

A downside of using μ CT for the structural analysis of freeze-dried products is the potential detrimental effect of X-ray radiation on product stability. The effects of relatively high radiation doses on APIs are widely studied for sterilization processes.^[8, 9] General recommendations based on these studies are not feasible, however. Differences in the susceptibility to radiation have been found within the same molecule class.^[10] Furthermore, radiation stability has been found dependent on API concentration.^[11, 12] Other formulation components can also influence the effect of ionizing radiation on product stability: surfactants such as polysorbate have been reported to provide a protective effect against radiation.^[12] While doses during μ CT scans are much lower, lower radiation doses do not necessarily lead to higher API stability.^[13] Unfortunately, very little information on the effect of low doses of X-ray radiation on API stability in the solid state is available: Uehara *et al.*^[14] subjected tablets of acetaminophen, loxoprofen, mefenamic acid, furosemide and nifedipine to X-ray radiation doses of up to 300 Gy and found no indication of significant differences in the drug content and only negligible colour differences for furosemide and nifedipine between irradiated and normal samples. Only one investigation of the stability of freeze-dried formulations subjected to low X-ray radiation doses has been found during the literature review: Vestergaard *et al.*^[15] irradiated freeze-dried recombinant activated factor VII formulations with X-ray doses of 0.4 and 2 mGy to simulate radiation exposure during airport security and flights. They also found no evidence of a detrimental effect on the API stability.

For the application of μ CT for the non-destructive inspection of freeze-dried products, stability is of utmost importance. This study aims to provide stability data for three different freeze-dried formulations subjected to μ CT analysis to complement the previous reports on low-dose X-ray exposure.^[14, 15] Three model compounds were subjected to X-ray doses of 100 Gy and analysed for stability to test the feasibility of using μ CT for structural analysis of freeze-dried products. The model compounds were chosen from three different classes of APIs based on previous reports on susceptibility to irradiation-induced damage. Clotrimazole was reported as unstable at typical sterilization doses and chosen as a small molecule compound.^[16, 17] Human insulin was chosen as a peptide compound. It has been reported as unstable when exposed to ionizing radiation.^[18, 19] Loss of activity and aggregation have been reported for L-lactate dehydrogenase (LDH) when exposed to ionizing radiation.^[20-22] The enzyme was chosen as a model protein. As commonly used in freeze-dried products with biological APIs, a surfactant was included in the insulin and LDH formulations.^[23, 24]

Materials and Methods

Materials

Clotrimazole, recombinant human insulin, methyl- β -cyclodextrin (average molecular weight of 1310 g/mol), anhydrous sodium sulfate, sodium azide, sodium pyruvate, reduced disodium β -nicotinamide adenine dinucleotide hydrate (NADH), polysorbate 20 (Tween 20), sucrose, monobasic sodium phosphate dihydrate, dibasic potassium phosphate, sodium hydroxide, potassium hydroxide, a protein standard mix for size exclusion chromatography (SEC) and ethanolamine were purchased from Sigma-Aldrich (Taufkirchen, Germany). Porcine LDH and phosphoric acid (85%) were purchased from Carl-Roth (Karlsruhe, Germany). Acetonitrile and methanol were purchased from Fisher Scientific; 2 M hydrochloric acid was purchased from Merck (Darmstadt, Germany).

Nipro PharmaPackaging 10-ml serum tubing vials (Münnerstadt, Germany) with 20-mm Westar RS stoppers and 20-mm Flip-Off seals by West (Eschweiler, Germany) were used for freeze-drying. Product temperatures were monitored with 36 AWG thin wire type T thermocouples (TCs, Omega Engineering, Deckenpfronn, Germany).

Methods

Formulation compounding

An overview of the formulation compositions is given in [Table 1](#). For solubility reasons, formulation 1 was adjusted to pH 2.5 with hydrochloric acid. The insulin for formulation 2 was first dissolved in 0.01 M HCl as recommended by the supplier. The solution was later adjusted to pH 4.5 with sodium hydroxide. Formulation 3 was

Table 1 Formulation compositions

Formulation	Substance	Concentration
1	Clotrimazole	0.1 mg/ml
	Methyl- β -cyclodextrin	7 mg/ml
	Sucrose	43 mg/ml
2	Insulin	1 mg/ml
	Polysorbate 20	0.5 mg/ml
	Sucrose	50 mg/ml
3	LDH	0.25 mg/ml
	Dibasic potassium phosphate	10 mM
	Polysorbate 20	0.5 mg/ml
	Sucrose	50 mg/ml

adjusted to pH 7.3 with potassium hydroxide. Each vial was filled with 2.5 ml which corresponds to a fill height of 0.7 cm.

Freeze-drying

Product vials were packed in a hexagonal packaging array with one row of 50-mg/ml sucrose placebo vials surrounding them. TCs were placed invasively at the bottom centre of two vials for each formulation. Freeze-drying was performed in a LyoStar 2 freeze-dryer (SP Scientific, Gardiner, NY).

Freezing was performed at -45°C shelf temperature with a 60-min hold time. During freezing, the shelf temperature was ramped with $1^{\circ}\text{C}/\text{min}$ with 45 min equilibration steps at 5 and -5°C to improve the homogeneity of ice nucleation temperatures.^[25] Primary drying was performed at -20°C shelf temperature with a ramp rate of $0.5^{\circ}\text{C}/\text{min}$ and at 20 mTorr chamber pressure. These conservative settings were chosen to minimize drying-induced defects in the products. The cycle was advanced into secondary drying when the Pirani pressure reading was identical to the capacitance manometer.^[26] The shelf temperature was ramped to $+40^{\circ}\text{C}$ with a ramp rate of $0.1^{\circ}\text{C}/\text{min}$ and held for 360 min during secondary drying.

Structural analysis, sample irradiation and accelerated stability storage

Vials were irradiated in a CTPortable System (Fraunhofer EZRT, Fuerth, Germany). The X-ray beam was hardened with a 2-mm aluminium filter. The current method used for structural analysis subjects the products to a maximum dose of approximately 10 Gy per scan. Scans of different model systems were performed to show examples of the structural information obtainable with these settings. A 70 mg/ml mannitol and 30 mg/ml S-adenosyl-L-methionine (SAM) formulation with a homogeneous cake structure and two 100 mg/ml SAM formulations with different internal structures were analysed. During the stability study, vials were irradiated with 100 Gy at 50 Gy/h to be on the safe side for future changes in the method or machine used for analysis. Vials not exposed to radiation were treated identically compared with the irradiated vials (e.g. kept in the same room for similar temperature exposure).

The stability of each model compound was assessed directly after freeze-drying and after set intervals of storage at 40°C and 75% relative humidity (4, 9 and 12 weeks).

Stability analysis

Stability was analysed with a Flexar HPLC system with a Series 200 UV/Vis detector and a Lambda 25 UV/Vis spectrometer (PerkinElmer, Rodgau, Germany). Three samples were analysed per time point and irradiation status (normal/irradiated). All samples were reconstituted in the solvent specified below and monitored for their reconstitution behaviour before analysis.

Formulation 1

The clotrimazole content was analysed by reversed-phase HPLC (RP-HPLC) with an InfinityLab Poroshell 120 EC-C18 column (Agilent, Waldbronn, Germany) with an inner diameter of 3 mm, 15 cm length and a particle size of 2.7 μm . Samples were dissolved in 10.0 ml of a 75:25 methanol and water mixture. The mobile phase was a 75:25 mixture of methanol and an aqueous solution with 4.4 g/l monobasic sodium phosphate dihydrate. The flow was set to 0.5 ml/min with a total runtime of 25 min per sample. Absorption at 254 nm was measured for quantification. A calibration curve over a concentration range of 10–30 $\mu\text{g}/\text{ml}$ was prepared for calculations; 20 μl was injected for each run. Every sample was analysed twice.

Formulation 2

Formulation 2 was analysed by RP-HPLC on the same column as formulation 1. Samples were dissolved in 10.0 ml of a 26:74 acetonitrile and water mixture. Solution A was prepared by dissolving 28.4 g anhydrous sodium sulfate in 1000 ml of water, adding 2.7 ml of 85% phosphoric acid and adjusting the pH to 2.3 with ethanolamine. A 26:74 acetonitrile and solution A mixture was used as the mobile phase. The flow was set to 0.7 ml/min with a total runtime of 50 min per sample. The detector measured the absorption at 214 nm. Insulin solutions over a concentration range of 10–30 $\mu\text{g}/\text{ml}$ were used for calibration. All solutions were stored at 4°C until injection. Twenty microlitres were injected for each run. Each sample was analysed twice.

Formulation 3

The stability of LDH was assessed by an activity assay and soluble aggregate content by SEC. Freeze-dried samples were dissolved in 2.5 ml of water and analysed. The activity measurements were performed as follows:

LDH catalyses the conversion between pyruvate and lactate with NADH/Nicotinamide dinucleotide + (NAD^+) as a cofactor. The consumption of NADH and thus the rate of this reaction can be assessed quantitatively by measuring the absorption over time at 340 nm.^[27] A reaction mixture with 0.15 mm NADH, 2 mm sodium pyruvate and a 10 mm potassium phosphate buffer with a pH of 7.3 was prepared. A 0.25 mg/ml LDH solution was prepared fresh as 100% activity reference. Three millilitres of the reaction mixture were pipetted into a 10-mm quartz cuvette. After the addition of 5 μl of LDH standard or sample solution, the absorption at 340 nm was measured over 60 s. Each sample was analysed in triplicate. Activity relative to the reference solution was obtained by comparing the slope of the absorption over time curves of the sample solutions to the reference measurements.

After UV analysis, the samples were transferred into chromatography vials and analysed by SEC. The samples were stored at 4°C until injection. A TSKgel G3000SWxl column (Tosoh Bioscience, Griesheim, Germany) with an inner diameter of 7.8 mm, 30 cm length and a particle size of 5 μm was used for separation. The mobile phase consisted of 15.6 g/l monobasic sodium phosphate dihydrate, 14.2 g/l sodium sulfate and 0.5 g/l sodium azide. The pH of the mobile phase was adjusted to 6.7 with sodium hydroxide. Twenty microlitres of samples were injected and analysed with a flow rate of 0.3 ml/min over a runtime of 40 min per sample. A 15–600 kDa protein standard mix was injected as a reference for retention times of higher molecular weight species. Eluents were quantified by absorption measurements at 280 nm. Each sample was analysed in duplicate. Soluble aggregate content is reported as percentage of the total peak area in the chromatograms.

Stability data analysis

The degradation of the API for content for formulations 1 and 2 (x_1 and x_2) or the loss of activity of LDH for formulation 3 (x_3) was analysed for reaction order by plotting $x_{1,2,3}$, $\ln x_{1,2,3}$ and $1/x_{1,2,3}$ against time and comparing the coefficients of determination (COD) for linear regression to test for zero-order, first-order and second-order kinetics, respectively.

The obtained stability data were subjected to a Kruskal–Wallis test. The hypothesis that the radiation exposure did not influence the content or activity was tested for the results at each time point of the stability study. The maximum H- and minimum P-values across the four different time points are reported for each formulation. P-values below 0.05 were considered statistically significant.

Results and Discussion

Structural analysis by μ CT

Scans of the 70 mg/ml mannitol and 30 mg/ml SAM (Figure 1a) and 100 mg/ml SAM model systems (Figure 1b and c) are shown to illustrate the structural information obtainable with the routine scan method. Figure 1a shows a homogeneous cake structure with no defects. Figure 1b shows a largely homogeneous pore structure with the exception of a small area near the bottom centre of the cake with larger pores and increased contrast. These higher contrast areas represent collapsed structures that are confined to the inside of the product and impossible to detect with a routine visual inspection.^{16, 71} The structure in Figure 1c features even larger pores and more pronounced collapse areas in the centre. A small layer near the top and sides of the product appears homogeneous and consequently conceals the defects on the inside.

The reader is advised that the spatial resolution of μ CT scans is dependent on the machine itself as well as the method used. Our goal during the method development of the structural analysis was to obtain information about structural defects such as collapsed areas, which can easily be distinguished by their higher contrast and larger pore sizes and the overall shape of the product. More in-depth information such as exact pore sizes requires higher resolution scans.

Freeze-drying

Product temperatures throughout primary drying were maintained below -37°C . TCs next to the 50 mg/ml sucrose placebo showed temperatures within 0.5°C compared with vials surrounded by the same formulation. Due to this insignificant difference, both vial

types were considered for stability analysis. The cycle was advanced into secondary drying after 48 h of primary drying.

Most of the product vials were considered pharmaceutically elegant with minimal shrinkage, which is expected for sucrose-based formulations.¹²⁸ Some vials of formulations 1 and 3 showed cracked cakes. No macroscopic differences between irradiated and non-irradiated samples could be observed. Only pharmaceutically elegant products without cracks were selected for the stability study.

Formulation 1

Reconstitution behaviour was identical for all samples. Peak areas of duplicate injections were found within 2% of each other (Figure 2a). The calibration solutions resulted in curves with CODs of at least 0.99 for each run. Example chromatograms of formulation 1 at 0 and 12 weeks are shown in Figure 3a and b, respectively. The clotrimazole signal is visible at 7.2 min. The formulation matrix shows a strong signal before the clotrimazole peak. Two main degradation products have been expected for clotrimazole: the substance has been reported to undergo hydrolysis to (2-chlorophenyl)-diphenylmethanol and imidazole during storage at acidic pH values and radiolysis to 1-(9-phenylfluoren-9-yl)-imidazole. The relative retention times of these impurities during RP-HPLC analysis compared with the clotrimazole signal are 0.9 and 1.7, respectively.¹¹⁶ The chromatograms in Figure 3a and b show no evidence of the radiolysis compound at higher retention times. The signals at lower retention times show that the formulation matrix is also degraded under the elevated temperature and humidity conditions. The magnitude of the matrix signal at lower retention times prevents the identification of clotrimazole degradation products in that region.

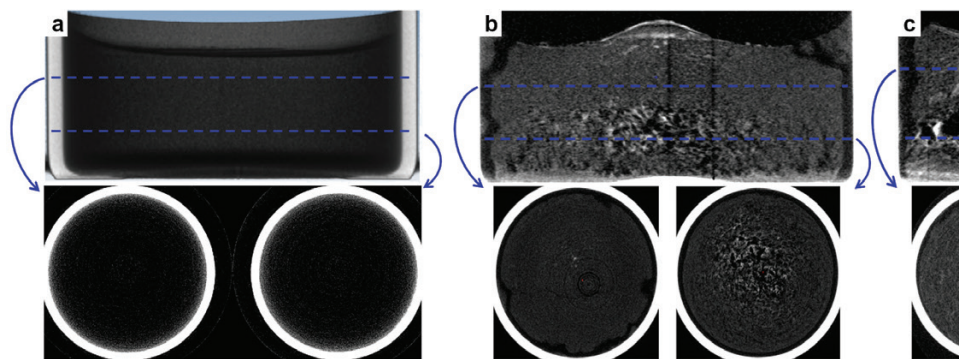


Figure 1 Example vertical section of the middle of the products and horizontal sections at two different heights by μ CT scans. Comparative images of a homogeneous 70 mg/ml mannitol and 30 mg/ml SAM product (a), a 100 mg/ml SAM product with minor collapse confined to the centre of the product (b) and a 100 mg/ml SAM product with large pores and pronounced collapse (c).

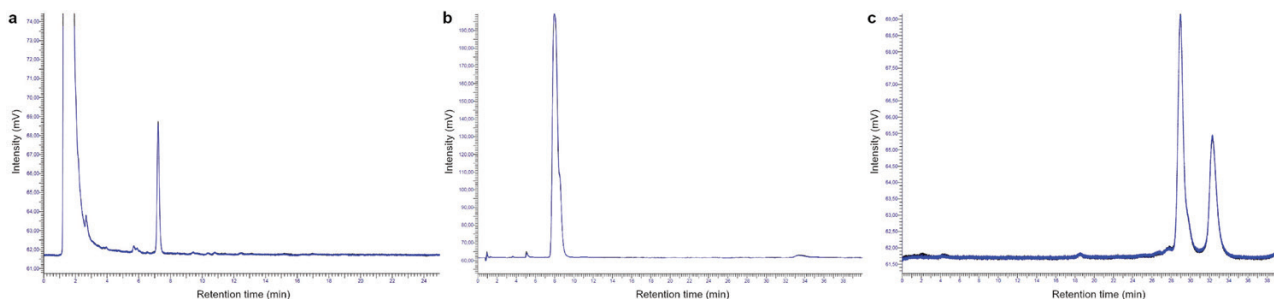


Figure 2 Example chromatograms obtained from duplicate injections of the same samples overlaid in blue and black for formulation 1 (a), 2 (b) and 3 (c) directly after freeze-drying.

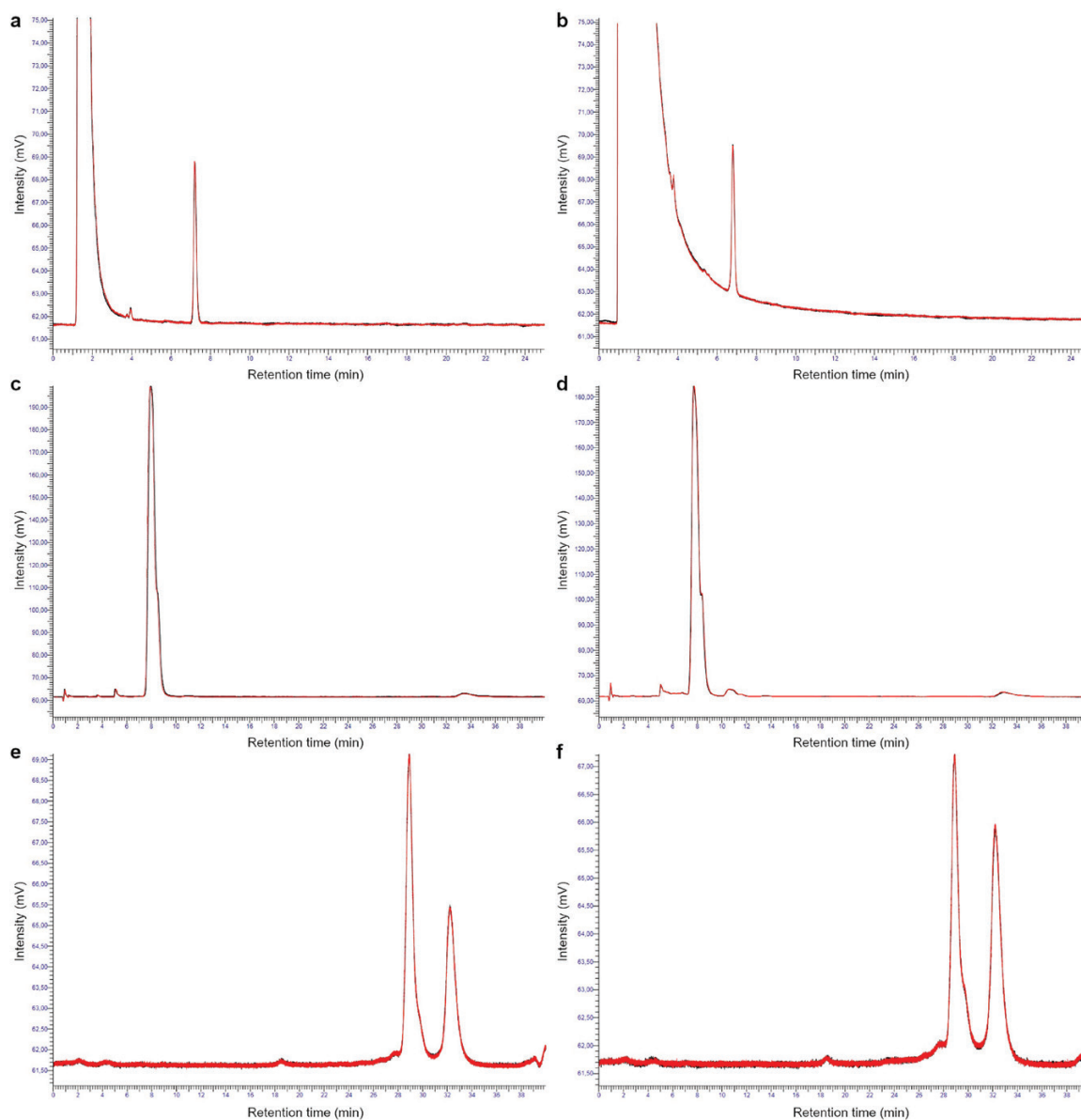


Figure 3 Overlays of normal sample chromatograms (black) and irradiated sample chromatograms (red) obtained directly after freeze-drying (a, c and e) as well as after 12 weeks of storage (b, d and f). Formulation 1: a and b; formulation 2: c and d; formulation 3: e and f.

Figure 4 shows the decline in clotrimazole content for the different time points and irradiation statuses investigated. Clotrimazole content directly after freeze-drying was found below 100%. This can likely be attributed to the stability reasons that suboptimal pH had to be used for sufficient solubility.^[29] The clotrimazole content decreased from approximately 97% directly after freeze-drying to 84% after 12 weeks of storage under elevated temperature and humidity conditions. The decrease over time can be described by zero-order or first-order kinetics. CODs for zero-order and first-order kinetics were 0.97 and 0.97 for normal and irradiated samples, respectively. Distinguishing between these is not feasible due to the low absolute content changes observed during the study. We hypothesize that a pseudo-first-order kinetic is more probable due to the main degradation pathway likely being the acid-catalysed hydrolysis of clotrimazole. The data clearly show that there is no significant difference in clotrimazole content for the irradiated samples compared with the samples not exposed to radiation ($H \leq 1.64$, $df = 1$, $P \geq 0.20$). The X-ray doses used in the

μ CT scans did not have a measurable influence on clotrimazole stability directly after freeze-drying or under accelerated stability conditions.

Formulation 2

No differences in the reconstitution behaviour could be observed for formulation 2. Reproducibility of duplicate injections was found within 2% of each other during the analysis of formulation 2 (Figure 2b). Calibration curves with CODs of at least 0.99 were achieved with the calibration solutions. Example chromatograms of formulation 2 at 0 and 12 weeks are provided in Figure 3c and d, respectively. Insulin was detected at 7.9 min. Insulin is expected to undergo aggregation after exposure to ionizing radiation and aggregation as well as deamidation to A-21 desamido insulin under elevated temperature and acidic pH values.^[19, 30] Soluble insulin aggregates have previously been reported at lower retention times compared with the insulin signal during RP-HPLC analysis.^[19] The signal at 10.6 min could be attributed to A-21

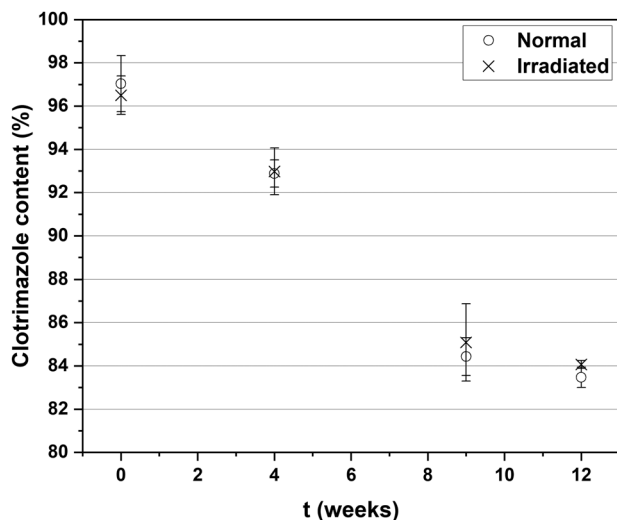


Figure 4 Clotrimazole content in formulation 1 over the course of the stability study. Error bars show standard deviation.

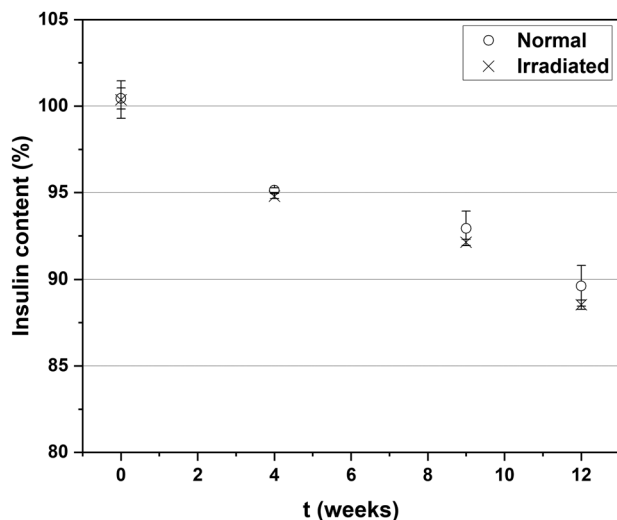


Figure 5 Insulin content in formulation 2 over the course of the stability study. Error bars show standard deviation.

desamido insulin. This was confirmed by dissolving insulin in 0.01 M hydrochloric acid and allowing it to stand at room temperature for 3 days to form at least 5% of A-21 desamido insulin as recommended in the United States Pharmacopeia (USP) insulin monograph to test the HPLC system suitability (data not shown).^[31] Comparison of the chromatograms shows an increase in the A-21 desamido insulin signal during the storage of the samples. Furthermore, the signal between 5 and 6 min shows a small increase, which could hint at a small fraction of soluble aggregates being formed during the storage of the formulation.

Figure 5 shows the results of the stability analysis for formulation 2. Insulin stability was maintained near 100% directly after freeze-drying. Over the course of the accelerated stability study, some degradation to a final insulin content of approximately 89% after 12 weeks can be observed. Kinetic analysis of the stability data shows a good correlation with zero-order or first-order kinetics (CODs for both reaction orders at 0.96 and 0.97 for normal and irradiated samples, respectively). Similar to clotrimazole, these

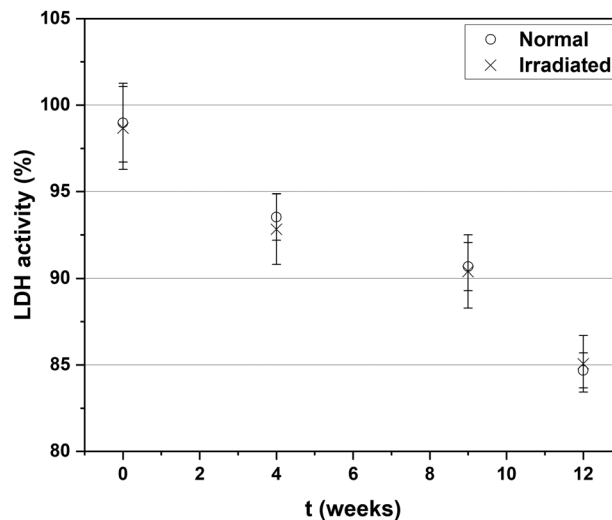


Figure 6 LDH activity in formulation 3 during the stability study. Error bars show standard deviation.

two cannot be clearly distinguished by mathematical analysis due to the low absolute content changes observed. Because the chromatograms confirmed the acid-catalysed degradation pathway to A-21 desamido insulin as the main degradation product, we hypothesize a pseudo-first-order type to be more likely for the degradation kinetics. Once again, the results of the analysis confirm no influence of the irradiation process on insulin stability: no significant differences between both types of samples could be observed over the course of the study ($H \leq 2.56$, $df = 1$, $P \geq 0.11$).

Formulation 3

Activity assay

Irradiated and normal samples showed no differences in their re-constitution behaviour. All absorption values measured during the activity assay were between 0.8 and 0.3 and showed a linear decline throughout the measurement. The results for formulation 3 can be seen in Figure 6. The activity assay showed that freeze-drying itself did not result in a significant loss of activity under the circumstances of this study. During storage, activity declined to a minimum of approximately 85% after 12 weeks of accelerated stability storage. Similar to the other formulations, this loss over time can be adequately described by zero-order (CODs 0.96 and 0.95 for normal and irradiated samples, respectively) or first-order kinetics (CODs 0.95 and 0.95 for normal and irradiated samples, respectively). More data, either over longer storage periods to cover lower activities or on the exact degradation pathway, would be necessary to formulate a substantiated hypothesis on the kinetics in this case. The comparison of irradiated and normal LDH samples showed no significant differences in activity over the course of the stability study, however ($H \leq 0.43$, $df = 1$, $P \geq 0.51$).

SEC

A chromatogram of the 15–600 kDa protein standard mix can be seen in Figure 7. The reader is advised that the peaks not labelled in the chromatogram are also present in the product information leaflet and likely correspond to by-products or multimers of the proteins used in the standard mixture. The chromatogram confirms the suitability of column and method for separation in the LDH size range. Two main peaks could be identified in the LDH chromatograms

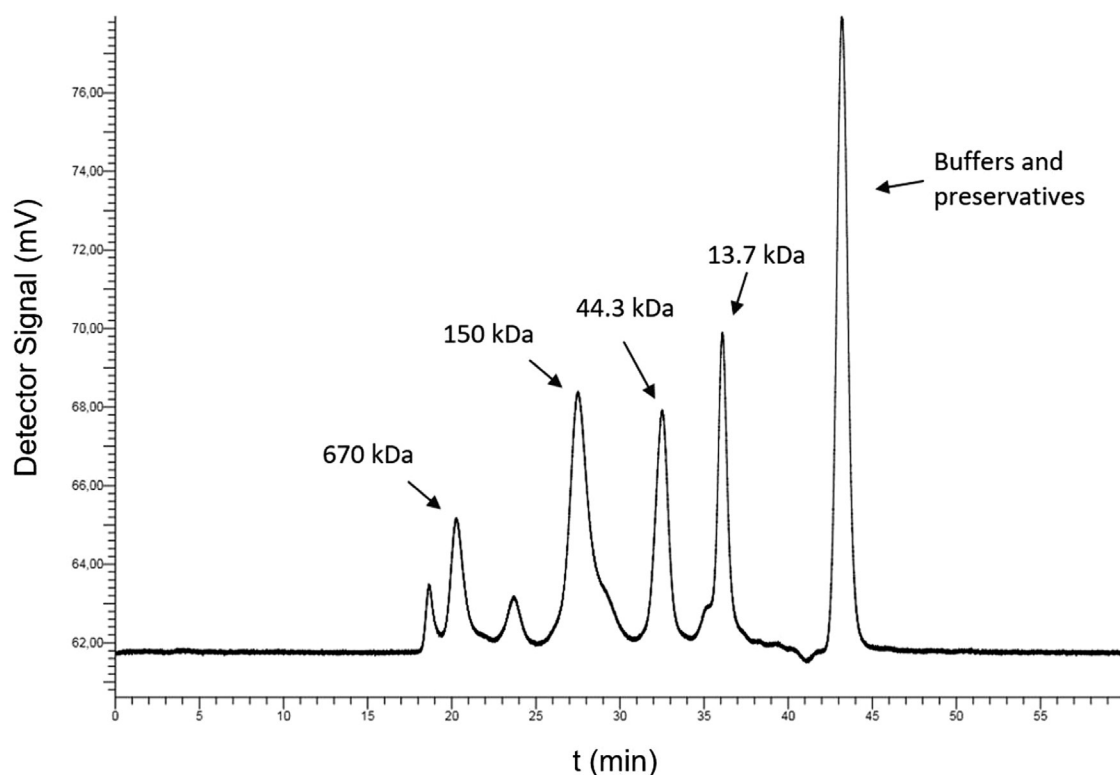


Figure 7 Chromatogram of the 15–600 kDa protein standard mix separation.

(Figure 2c). By comparison of retention times with the standard mix, these signals could be attributed to the LDH tetramer (140 kDa at 29.0 min) and its dimer (70 kDa at 32.2 min). These two forms of the enzyme are known to be in a concentration-dependent equilibrium in an aqueous solution.^[32] Figure 3e and f shows example chromatograms of formulation 3 directly after freeze-drying and after 12 weeks of storage, respectively. Apart from the main signals, aggregates peaks have been found between 18 and 28 min. Additionally, a decrease in the tetramer to dimer ratio can be observed after 12 weeks of storage.

The overview of soluble aggregates during the stability study is shown in Figure 8. The freeze-drying process itself led to approximately 2% of soluble aggregates being formed. In contrast to the results of the activity assay, the formulation remained largely stable throughout the stability study regarding aggregate formation. Only a small trend toward larger aggregate contents can be seen after 12 weeks of aggressive storage conditions. The stable aggregate content as well as a lower tetramer-to-dimer ratio could hint at structural changes in the enzyme that compromise activity while maintaining size.

Data comparison between irradiated and normal samples, however, leads to the same conclusion as the activity assay: radiation exposure of formulation 3 did not lead to a significant increase in soluble aggregate formation as measured by SEC ($H \leq 1.26$, $df = 1$, $P \geq 0.26$).

Limitations of the study

This study focussed on the evaluation of API stability directly after freeze-drying and storage at high temperature and humidity conditions. The storage aspect was an important part of the investigation because of the tendency of ionizing radiation to form highly reactive

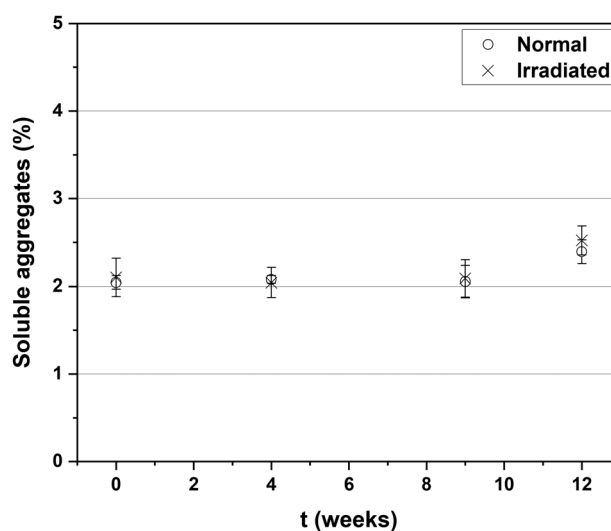


Figure 8 Soluble aggregates of LDH in formulation 3 determined by SEC. Error bars show standard deviation.

chemical species such as radicals or ions.^[33] Some radicals have been reported to persist in the solid state.^[34] The presence of these species could lead to a relatively late manifestation of a detrimental effect by ionizing radiation, especially because of the low molecular mobility in the dried products.^[35] Detection of ion or radical degradation products would have been possible by electro spin resonance spectroscopy^[36, 37] but was not in the scope of this study because of the questionable pharmaceutical relevance of trace amounts of these substances.

The reader is advised that this study only aims to provide exemplary data for different molecule classes as a proof of concept for the safety of small X-ray systems to be used for the structural analysis of freeze-dried products. The evaluation of structural information as well as the quantification of defect severity from such a small μ CT system is part of an ongoing investigation.

Conclusions

The results show that the three model compounds were maintained in good conditions directly after freeze-drying. As expected, over the course of the storage duration, some degradation of all compounds could be seen due to the high temperature and humidity conditions. Differences between the irradiated and normal state could not be distinguished for all three model compounds. While larger doses than the 100 Gy tested may lead to radiation-induced degradation, these are not expected to be reached during routine structural analysis with the current setup since that would require scan times of more than 2 hours per sample.

This study confirms that the X-ray doses used for structural analysis may not be problematic for pharmaceutical APIs, which have previously been reported as susceptible to radiation-induced damage. Due to the small sample size in this study and the vast chemical and biological heterogeneity of pharmaceutical APIs, individual stability should still be evaluated on a case-by-case basis if μ CT is considered as an option for non-destructive inspection.

Acknowledgement

The authors would like to thank the Division of Pharmaceutics (LPT) of Friedrich-Alexander University (FAU) Erlangen Nuernberg for the analytical support.

Funding

Medac, Wedel, Germany, is gratefully acknowledged for partially funding this study.

Author Contributions

H.G., T.P. and S.S.-L. had the idea for the present study and designed the experiments. T.W., A.S. and P.M. performed the experimental work, analysed the raw data and helped to interpret the data set. T.W. and H.G. solely wrote the manuscript, but in consultation with S.S.-L. and T.P.

Conflict of Interest

The authors declare that there is no conflict of interest.

References

- Pisano R, Arsiccio A, Nakagawa K *et al.* Tuning, measurement and prediction of the impact of freezing on product morphology: a step toward improved design of freeze-drying cycles. *Dry Technol* 2019; 37: 579–99. <https://doi.org/10.1080/07373937.2018.1528451>
- Assegehegn G, Brito-de la Fuente E, Franco JM *et al.* The importance of understanding the freezing step and its impact on freeze-drying process performance. *J Pharm Sci* 2019; 108: 1378–95. <https://doi.org/10.1016/j.xphs.2018.11.039>
- Meister E, Gieseler H. Freeze-dry microscopy of protein/sugar mixtures: drying behavior, interpretation of collapse temperatures and a comparison to corresponding glass transition data. *J Pharm Sci* 2009; 98: 3072–87. <https://doi.org/10.1002/jps.21586>
- Patel SM, Nail SL, Pikal MJ *et al.* Lyophilized drug product cake appearance: what is acceptable? *J Pharm Sci* 2017; 106: 1706–21. <https://doi.org/10.1016/j.xphs.2017.03.014>
- Pisano R, Barresi AA, Capozzi LC *et al.* Characterization of the mass transfer of lyophilized products based on X-ray micro-computed tomography images. *Dry Technol* 2017; 35: 933–8. <https://doi.org/10.1080/07373937.2016.1222540>
- Haeuser C, Goldbach P, Huwyler J *et al.* Imaging techniques to characterize cake appearance of freeze-dried products. *J Pharm Sci* 2018; 107: 2810–22. <https://doi.org/10.1016/j.xphs.2018.06.025>
- Kunz C, Schuldt-Lieb S, Gieseler H. Freeze-drying from organic co-solvent systems, part 2: process modifications to reduce residual solvent levels and improve product quality attributes. *J Pharm Sci* 2019; 108: 399–415. <https://doi.org/10.1016/j.xphs.2018.07.002>
- Silindir M, Ozer Y. The effect of radiation on a variety of pharmaceuticals and materials containing polymers. *PDA J Pharm Sci Technol* 2012; 66: 184–99. <https://doi.org/10.5731/pdaipst.2012.00774>
- Sarcant ET, Ozer AY. Ionizing radiation and its effect on pharmaceuticals. *J Radioanal Nucl Chem* 2020; 323: 1–11.
- Mercanoglu GO, Ozer AY, Colak S *et al.* Radiosterilization of sulfonamides: I: determination of the effects of gamma irradiation on solid sulfonamides. *Radiat Phys Chem* 2004; 69: 511–20. <https://doi.org/10.1016/j.radphyschem.2003.09.005>
- Nisar J, Sayed M, Khan FU *et al.* Gamma – irradiation induced degradation of diclofenac in aqueous solution: kinetics, role of reactive species and influence of natural water parameters. *J Environ Chem Eng* 2016; 4: 2573–84. <https://doi.org/10.1016/j.jece.2016.04.034>
- Bosela AA, Salamah KK, Alsarra IA *et al.* Reactivity of prednisolone to gamma radiation in aqueous and organic solutions. *J Drug Deliv Sci Technol* 2010; 20: 225–9. [https://doi.org/10.1016/S1773-2247\(10\)50034-0](https://doi.org/10.1016/S1773-2247(10)50034-0)
- Blue RS, Chancellor JC, Antonsen EL *et al.* Limitations in predicting radiation-induced pharmaceutical instability during long-duration spaceflight. *NPJ Microgravity* 2019; 5: 15. <https://doi.org/10.1038/s41526-019-0076-1>
- Uehara K, Tagami T, Miyazaki I *et al.* Effect of X-ray exposure on the pharmaceutical quality of drug tablets using X-ray inspection equipment. *Drug Dev Ind Pharm* 2014; 41: 953–8. <https://doi.org/10.3109/03639045.2014.917093>
- Vestergaard S, Nedergaard H, Jonasdottir O *et al.* Effect of X-ray radiation exposure on lyophilized recombinant activated factor VII (formulated for storage at room temperature). *Curr Med Res and Opin* 2009; 25: 2699–702. <https://doi.org/10.1185/03007990903299705>
- Marciniec B, Dettlaff K, Naskrent M. Influence of ionising irradiation on clotrimazole in the solid state. *J Pharm Biomed Anal* 2009; 50: 675–8. <https://doi.org/10.1016/j.jpba.2008.08.032>
- Marciniec B, Kozak M, Dettlaff K. Thermal analysis in evaluation of the radiochemical stability of some fungicidal drugs. *J Therm Anal Calorim* 2004; 77: 305–17. <https://doi.org/10.1023/B:JTAN.0000033215.77806.b0>
- Kopoldová J. Radiation aggregates of insulin. *Z Naturforsch C Biosci* 1979; 34: 1139–43. <https://doi.org/10.1515/znc-1979-1210>
- Terry H, Maquille A, Houée-Levin C *et al.* Irradiation of human insulin in aqueous solution, first step towards radiosterilization. *Int J Pharm* 2007; 343: 4–11. <https://doi.org/10.1016/j.ijpharm.2007.04.012>
- Winstead JA, Reece TC. Effects of gamma radiation on the chemical and physical properties of lactate dehydrogenase. *Radiat Res* 1970; 41: 125–34. <https://doi.org/10.2307/3572901>
- Gupta GS, Kang BPS. Molecular and kinetic properties of sperm specific LDH after radiation inactivation. *Mol Cell Biochem* 2000; 206: 27–32. <https://doi.org/10.1023/A:1007037128143>
- Hategan A, Martin D, Popescu LM *et al.* Effects of radiation on frozen lactate dehydrogenase. *Bioelectrochemistry* 2001; 53: 193–7. [https://doi.org/10.1016/s0302-4598\(00\)00131-8](https://doi.org/10.1016/s0302-4598(00)00131-8)
- Emami F, Vatanara A, Park EJ *et al.* Drying technologies for the stability and bioavailability of biopharmaceuticals. *Pharmaceutics* 2018; 10: 131. <https://doi.org/10.3390/pharmaceutics10030131>
- Authelin JR, Rodrigues MA, Tchessalov S *et al.* Freezing of biologicals revisited: scale, stability, excipients, and degradation stresses. *J Pharm Sci* 2020; 109: 44–61. <https://doi.org/10.1016/j.xphs.2019.10.062>

25. Tang X, Pikal MJ. Design of freeze-drying processes for pharmaceuticals: practical advice. *Pharm Res* 2004; 21: 191–200. <https://doi.org/10.1023/B:PHAM.0000016234.73023.75>
26. Patel SM, Doen T, Pikal MJ. Determination of end point of primary drying in freeze-drying process control. *AAPS PharmSciTech* 2010; 11: 73–84. <https://doi.org/10.1208/s12249-009-9362-7>
27. Al-Hussein A, Gieseler H. The effect of mannitol crystallization in mannitol-sucrose systems on LDH stability during freeze-drying. *J Pharm Sci* 2012; 101: 2534–44. <https://doi.org/10.1002/jps.23173>
28. Ullrich S, Seyferth S, Lee G. Measurement of shrinkage and cracking in lyophilized amorphous cakes. Part I: final-product assessment. *J Pharm Sci* 2015; 104: 155–64. <https://doi.org/10.1002/jps.24284>
29. Tawakkol SM, Fayez YM, Fahmy NM *et al.* Monitoring of clotrimazole degradation pathway in presence of its co-formulated drug. *J Chromatogr Sci* 2019; 57: 518–27. <https://doi.org/10.1093/chromsci/bmz024>
30. Moslemi P, Najafabadi AR, Tajerzadeh H. A rapid and sensitive method for simultaneous determination of insulin and A21-desamido insulin by high-performance liquid chromatography. *J Pharm Biomed Anal* 2003; 33: 45–51. [https://doi.org/10.1016/s0731-7085\(03\)00336-4](https://doi.org/10.1016/s0731-7085(03)00336-4)
31. USP 42–NF 37: Insulin Monograph. *The United States Pharmacopeia and National Formulary*. Weilheim, Germany: Deutscher Apotheker Verlag, 2019.
32. Andrews BA, Dyer RB. Small molecule cores demonstrate non-competitive inhibition of lactate dehydrogenase. *Med Chem Commun* 2018; 9: 1369–76. <https://doi.org/10.1039/C8MD00309B>
33. Varshney L, Dodke P. Radiation effect studies on anticancer drugs, cyclophosphamide and doxorubicin for radiation sterilization. *Radiat Phys Chem* 2004; 71: 1103–11. <https://doi.org/10.1016/j.radphyschem.2003.12.052>
34. Vallotto C, Williams HE, Murphy DM *et al.* An electron paramagnetic resonance (EPR) spectroscopy study on the γ -irradiation sterilization of the pharmaceutical excipient l-histidine: regeneration of the radicals in solution. *Int J Pharm* 2017; 533: 315–19. <https://doi.org/10.1016/j.ijpharm.2017.09.068>
35. Yoshioka S, Aso Y. Correlations between molecular mobility and chemical stability during storage of amorphous pharmaceuticals. *J Pharm Sci* 2007; 96: 960–81. <https://doi.org/10.1002/jps.20926>
36. Polat M, Korkmaz M. ESR detection and dosimetric properties of irradiated naproxen sodium. *Int J Pharm* 2003; 255: 209–15. [https://doi.org/10.1016/s0378-5173\(03\)00080-2](https://doi.org/10.1016/s0378-5173(03)00080-2)
37. Aydaş C, Polat M, Korkmaz M. Identification and dosimetric features of γ -irradiated cefadroxil by electron spin resonance. *Radiat Phys Chem* 2008; 77: 79–86. <https://doi.org/10.1016/j.radphyschem.2007.02.077>